*Aquatic Mammals* 1990, **16.3**, 145–155

# The use of computed tomography in cetacean research Airsac determination of *Lagenorhynchus albirostris*; Part 1

Maria E. L. Brouwers, C. Kamminga*

*Information Theory Group, Delft University of Technology, P.O. Box 5031, 2600 GA Delft, Netherlands*

A. I. J. Klooswijk

*Radiodiagnostics Group, Erasmus University Rotterdam, Netherlands*

R. P. Terry

*Information Theory Group, Delft University of Technology, Netherlands*

**Abstract**

The use of x-ray computed tomography can be a powerful tool in research on cetaceans in general. The computed tomography scanner makes digital images corresponding to slices of a subject. These images give a representation of the different tissues within the slice. The different densities of the tissues are converted into corresponding density values. Relatively simple image processing techniques can be used to select a homogeneous region within a series of images and to calculate the contours, sizes and shape characteristics of the region. This is an improvement over classical anatomical techniques, where anatomical features like airsac dimensions are imprecisely determined. The images can be stored on tape and used over and over again. The computed tomography scanner does not damage the specimen, so further experiments using the same animal can be done after scanning.

The present study deals with the nasal tract system of the White-beaked dolphin (*Lagenorhynchus albirostris*), of which area and contents from adjacent slices are calculated. Three-dimensional reconstructions can be made to get a better overall idea of the nasal tract system in order to identify this biomechanical system as a candidate for sonar sound production. Due to the post-mortem condition of the head, the nasal tract system under investigation did not give an exact mapping of the actual shapes.

## Introduction

Over the last thirty years, research into the source of the high-frequency sound, or sonar, that odontocetes produce has slowly accumulated. Experts are still not in agreement concerning the anatomical source of these signals. All of the information gathered to date has tended to lump the theory of sound production into two camps, each with its own adherents and arguments in favour of its own hypothesis.

One group pinpoints the larynx as the source of sound production (see Fig. 1). Its arguments suggest that no air can escape when the sounds are produced in the larynx (Lawrence & Schevill, 1956). The sound is then easily transported by the palatopharyngeal sphincter muscles and the bones of the skull to the rostrum or the melon (Purves & Pilleri, 1978; Pilleri, 1979). The sound would be produced by pressing small quantities of air, under muscular control, through three slits at the apex of the larynx, which create the sound through a stretching and relaxing mechanism. The air could be stored and re-cycled through the premaxillary sacs or the caudal nasofrontal sacs (Schenkkan, 1972). The sound would finally travel through the maxilla and be emitted in a tight beam pattern through the upper jaw (Pilleri, 1979). The main function of the air-sac system would be as a sealing mechanism with possibly a secondary function of reflecting sounds from below (Schenkkan, 1977).

Opponents of this hypothesis argue that the slits at the apex of the larynx of a cetacean do not resemble the vocal cords of other mammals (Parry, 1978). As acoustic vibrations are highly attenuated during bone propagation, sound transmission by internal bone conduction, as suggested above, has been refuted (Alcuri, 1980). Moreover, no pressure differences were measured in the larynx of a dolphin during sound production (Ridgway *et al.*, 1980).

*All correspondence should be directed to the second author.

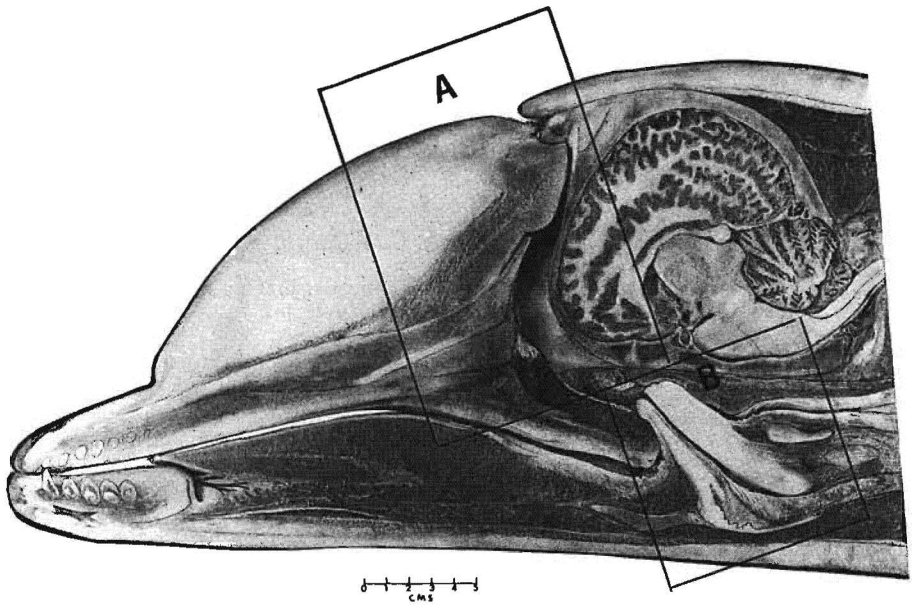


**Figure 1.** Midsagittal section through the head of *Tursiops truncatus*. A. Nasal area. B. Laryngeal area.

A second group of researchers believes the sound is produced in the nasal tract complex of the dolphin (see Figs 1 and 2). The exact source within the nasal tract is still under discussion.

Originally the right nasal plug was mentioned as the source of sound production (Norris *et al.*, 1972; Dormer, 1979). The plug would bounce or vibrate, under muscular control, against the hard edge of the bony nares as air is passed between the plug and the nasal walls (Evans & Maderson, 1973). Lipids in the nasal plugs have also been mentioned as the source of the sonar. This argument is supported by ultrasound measurements (Mackay & Liaw, 1981). During these experiments it was found that the nasal plugs vibrate synchronously with the sonar clicks, the right plug continuously and the left occasionally.

Another possible source of sound in this region are the 'museau de singe' (Norris, 1964). These structures are near the vestibular sacs and they would work like the lips of a trumpeter (see Fig. 3). The sounds produced by relaxation of the lips of the museau de singe would be transported by the dorsal bursae (Cranford, 1988) through the melon to be focused into a directional beam (Evans & Prescott, 1962). Opponents of this hypothesis believe that there is insufficient muscular control and too much air consumption near the museau de singe for sonar production to take place (Schenkkan & Purves, 1973).

Further, opponents of the nasal tract region as a sound source believe that air passing the nasal plugs for use in sound production would probably interrupt the closure of the blowhole (Schenkkan, 1972). They argue, in addition, that since the bony nares vary greatly in form and development, even within a subgroup, that the airsac region is an unlikely source of the sounds.

The true source of sonar emission still remains a matter of educated speculation and supposition and experts in the study of odontocetes continue to disagree about the source of sonar. Traditionally research, on which the theories of sound production are based, has been done through anatomical studies. Recently, innovative approaches to the problem using ultrasound, photography, electromyographic and pressure changes have been used. The use of other modern techniques will be important in advancing research in this area.

Information about the position, shape, contents and elasticity of the airsacs can be used to find out if it is physically possible for the production of sonar to occur in the nasal tract region. In the past, the airsacs have been measured by dissection of deceased dolphins. It is very likely that the airsacs deform or collapse during the dissection. Using a CT-scanner this problem disappears. The specimen remains in its original condition and images representing a slice of the mammal approximately 1 mm in thickness can be made. The use of x-ray computed tomography (CT) as an investigative tool with odontocetes has already been demonstrated (Cranford, 1988).

## Materials

The scans were made using a Philips Tomoscan T350. Scanning protocol was 120 kV and 120 mA

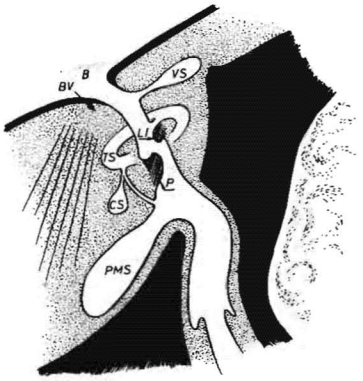


**Figure 2.** Diagram of the nasal tract (after Dudok van Heel). B = blowhole, VS = vestibular sac, CS = connecting sac, TS = nasofrontal sac, PMS = premaxillary sac, P = nasal plug.

with an exposure time 2.4 sec in 3 mm thick slices. The images were stored in coded format on a disk. At the Delft University of Technology the images were loaded into a VAX 11/750 of the Information Theory Group. The number of density values remained 4096. The images used had 256 pixels* in horizontal and vertical directions. A series of 22 images of the same scale covering the whole nasal tract region was used. The distance between two successive images was 3 mm (see Fig. 4). The pixel surface in the images was in reality 0.36 $mm^2$. This means that the surface of a whole image is 235.93 $cm^2$.

A CT-scanner probes a slice of a body using x-rays beamed from different directions. Between the x-ray tube and the detector system of the CT-scanner, the slice of the body is explored. Usually this slice is perpendicular to the main axis of the body.

X-rays sent through a body are absorbed by the compact structure of bone and penetrate better through the softer tissues. A circular array of detectors collects the penetrated x-rays. The absorbtion data, as obtained by the detectors, are stored in a computer. The system rotates over a small angle around the body and new measurements are performed. In this way data from different angles along a plane are collected. Finally, all collected data are used to reconstruct the slice.

The image constructed shows the different tissues and structures in different shades between black and white. There are 4096 varying shades or density values. The density value of a tissue depends on the density of the tissue. The less dense the tissue the darker the shade. For visual inspection on a screen the number of density values is reduced to a number of 256 grey levels. The representation of the image is accomplished by using the Hounsfield numbers (see Table 1).

The Hounsfield numbers are between −1000 and 3095. Often 1000 is added to get only positive numbers. The higher the number, the lighter the shade in the image. Air will be black, bone will be white. When two regions with different Hounsfield numbers and at least two millimetres in diameter, they can be separated. In general the resolution also depends on the thickness of the slice. The thinner the slice, the better the two regions can be separated. The thinnest slice is around 1 millimetre. For a detailed description of computed tomography measurements the reader is referred to Kak & Slancy, 1988.

The subject under investigation in this research was a White-beaked dolphin (*Lagenorhynchus albirostris*). The female animal (TL 2.80 m) was accidently caught in a fishing net and drowned in the North Sea. It was frozen immediately after being brought ashore. Scanning of the frozen subject took place at the University Hospital of the Erasmus University Rotterdam on 17 June, 1987.

A dolphin has two nasal channels between the blowhole and the bony nares. There are a number of airsacs along these channels. Most dolphins have four pairs of airsacs along the nasal channels: the vestibular sacs, the nasofrontal sacs, the connecting sacs and the premaxillary sacs (see Fig. 5A). The airsac pairs are asymmetrical. Usually the right sacs are larger than the left ones. How large the difference is depends on the species (see Fig. 5B).

The vestibular sacs, just below the skin along the nasal channels, are often seen as extensions of the vestibule. Microscopic analysis has shown that these sacs regularly shrink and expand.

The next pair of sacs, the nasofrontal sacs, are tubular in shape and are therefore sometimes called tubular sacs. They are nearly horizontal within the head and only have a small opening to the nasal channels.

Not all dolphins have connecting sacs. For this reason they are sometimes called accessory sacs. They are situated along the caudal wall of the nasal channels, ventral to the opening of the nasofrontal sacs with which they are connected.

The last pair of sacs are the premaxillary sacs. These are situated on the smooth part of the premaxilla, close to the opening of the bony nares. These are the largest sacs.

## Methods

Figure 6 illustrates a typical example of a delphinid CT-scan. The airsacs appear as blue regions in the images. It is difficult to find the exact boundaries of these regions by visual inspection. The boundary is important in determining the shape and the surface of an airsac. A method to find the exact

*Picture Elements.

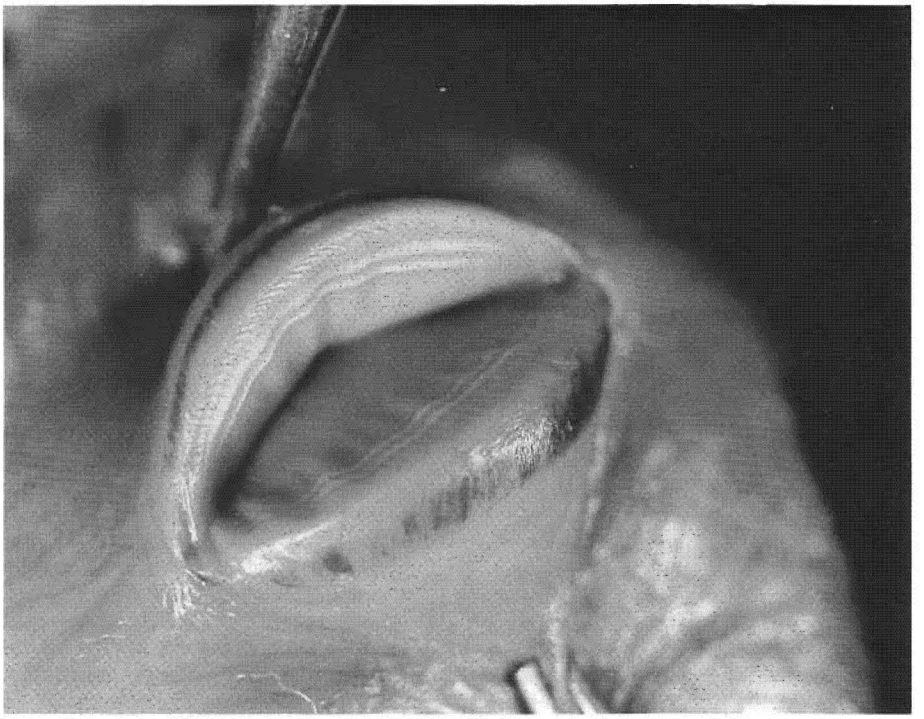

**Figure 3.** Example of the lips of the 'museau de singe' of the right nares (*Kogia* spp). The lips have been drawn apart to show the structure of the interior walls (From Schenkkan & Purves, 1973, with kind permission of the editor).

boundary should be easy but should always give a closed contour, as close to the real contour as possible. A contour is defined as a one-pixel boundary between an area with homogeneous properties and its surroundings with different properties.

Contours in the images can be found precisely using the threshold method. This method uses the characteristic ability of the CT-scanner to give tissues with a different density a different shade. Air has the lowest density value of 0. When all pixels with a density value below a certain threshold are selected, all of the air regions and some spurious noise pixels with density values above the threshold (of background noise) are selected. The cross-section of the airsac is found by taking the largest surface within a restricted area. The pixels at the boundary of the surface form the contour.

The choice of the threshold has a great influence on the location of the contour. The higher the threshold, the larger the surface. The distribution of the density values in and around the air surface are in a wide range of density values. The density values in the images are between 0 and 4095. In the centre of an airsac, the density value is below 100. Around this centre there is a region with density values between 100 and 900. All density values occur to the same small degree. Above the level of 900, the number of pixels in each density value is larger. In the region next to the air surface, the density values of the pixels are all between 900 and 1100. This means that the threshold should be below 900. A threshold of 850 was found by visual inspection to be the best choice. Figure 6 indicates the contour of the right vestibular sac as an example. An explanation for the wide range of density values found near the boundary of an air surface is the shape of the walls of an airsac. These walls are very wrinkled, which means that air and tissue very often alternate. This can create a density value between the air and the tissue level.

The 22 images used in the study had the same scale and were made from a dolphin in one position. This means that they link up with each other. Within an image, there was usually more than one airsac, but the contour of only one airsac at a time was calculated. This was done for all of the images showing the airsac. To select from which airsac the contours should be determined, a search region was selected in one of the images. In this selected region, the airsac from which the contour would be determined should have the largest air surface. Selecting a region is

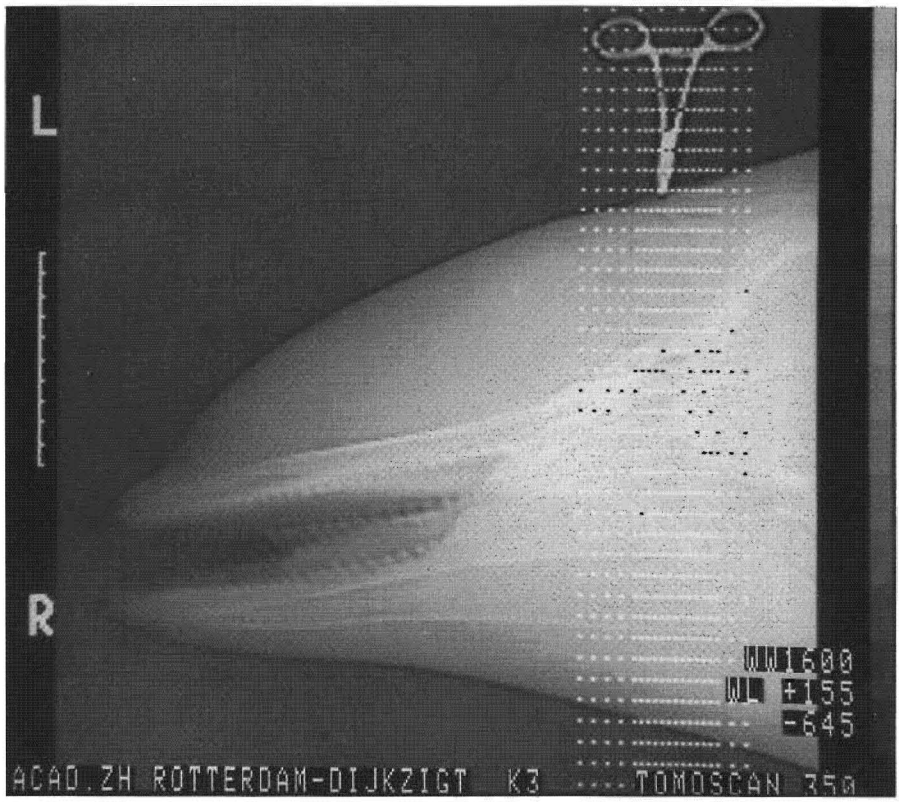


**Figure 4.** Sagittal cross-section of a *Lagenorhynchus albirostris*. The blowhole is indicated by a pair of scissors. The region of interest is marked by the dotted lines.

**Table 1.** The Hounsfield numbers of several materials

| | |
|---|---|
| Air | −1000 |
| Fat | −100 |
| Water | 0 |
| Blood | 12 |
| White brain tissue | 22–32 |
| Grey brain tissue | 36–46 |
| Congealed blood | 55–75 |
| Compact tumour tissue | 50–90 |
| Bone | 200–1000 |
| Compact bone | up to 3095 |

especially easy for large airsacs. In the other images, a new search region was selected automatically by the computer using the contour found in the previous image as a reference. All pixels within a certain distance from the contour will be in the next search region.

After a contour was found, the geometrical properties were described by calculating four shape characteristics: perimeter, area, dispersion and the elongation of the cross-section. To obtain the different shape characteristics, chain coding (Rosenfeld & Kat, 1982, ch. 1) was used.

To estimate the perimeter of the contour, the relative length of the line segment between each two pixels is calculated. The chain code employs only horizontal and vertical line sequents (and has an even number) together with diagonal line segments (old numbers). Following Vossepoel & Smeulders (1981) the perimeter is then given by

$$P = 0.948\ N_E + 1.340\ N_0$$

The actual real perimeter is found by multiplying the calculated number by the real distance (0.06 mm).

To estimate the area, the number of pixels on and within the contour is counted. This number, multiplied by the real area of a pixel (0.36 $mm^2$) gives the real area of the air region.

The dispersion gives information about the complexity of a shape. When the perimeter is small compared to the area, the object is relatively compact

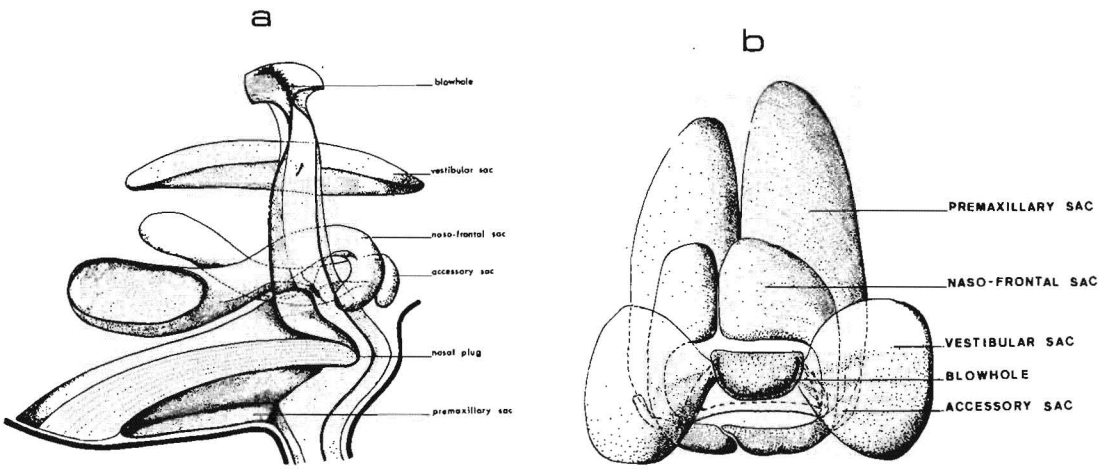


**Figure 5.** a. Diagram of the medial view of the right part of the nasal tract and its diverticulae in *Lagenorhynchus albirostris*. b. Diagram of the dorsal view of the nasal tract and its diverticulae in *L. albirostris* (From Schenkkan, 1971, with kind permission of the editor).

(for example a circle). When the perimeter gets larger compared to the area, the object is spread out. The measure of dispersion is given by:

$$\text{dispersion} = p^2/A.$$

The last shape characteristic that is calculated is the elongation. To find the elongation, the thickness t is compared to the area A. When the area is large compared to the thickness, the object will be very elongated, e.g. a long narrow rectangle will be much more elongated than a square. The elongation is given by:

$$\text{elongation} = A/t^2$$

The result of the calculation of the elongation is very different from the result of the calculation of the dispersion. A circle with a wrinkled boundary will have a large dispersion but a quite low elongation, although the elongation will be larger than the elongation of a smooth circle (Rosenfeld & Kak, 1982).

The surface area of the whole airsac was approximated by adding all perimeters—as calculated from all contours—multiplied by the image distance (3 mm). The contents of the airsac was approximated by adding all areas multiplied by the image distance.

To get a better idea of the shape of the airsac, it is possible to look at the airsacs from another direction. The original images were made from a posterior line-of-sight along the body axis. There are eight other standard lines-of-sight defined (see Fig. 7). Apart from that, an arbitrary line-of-sight direction in between the standard lines-of-sight can be chosen. The new image is constructed in such a way that the distance between two pixels is equal horizontally and vertically. The distance between two images is usually larger than between two pixels. Part of the new image is found by interpolation. The contours detected in the original images can be seen along the same lines-of-sight. These contours can be best used in combination with the reconstructed images. In some directions, the original images ought to be rotated before performing the reconstruction. This rotation takes a lot of computing time.

A better total view is given when the whole airsac is shown. This can be done by using a perspective view. A viewing point with an aperture is chosen. The contours are placed in a coordinate system with its origin in the centre of the object. This centre is approximated by the central point of the middle contour. When this point is not in the real centre, the reconstruction does not appear in the centre of the screen. The reconstruction is accomplished after transforming the coordinate system to the viewing point. The original contour pixels are transformed separately in such a way that the object appears in perspective on the screen. The view depends on the viewing point and the aperture. The view never fully represents reality, but because the eye also views perspectively, it is a good approximation. To see the depth more clearly, the distant contours have a lower density value than the closer contours, which are more clearly distinguished from the background.

## Results

Due to insufficient computer programmes available at the time this research was conducted, the desired

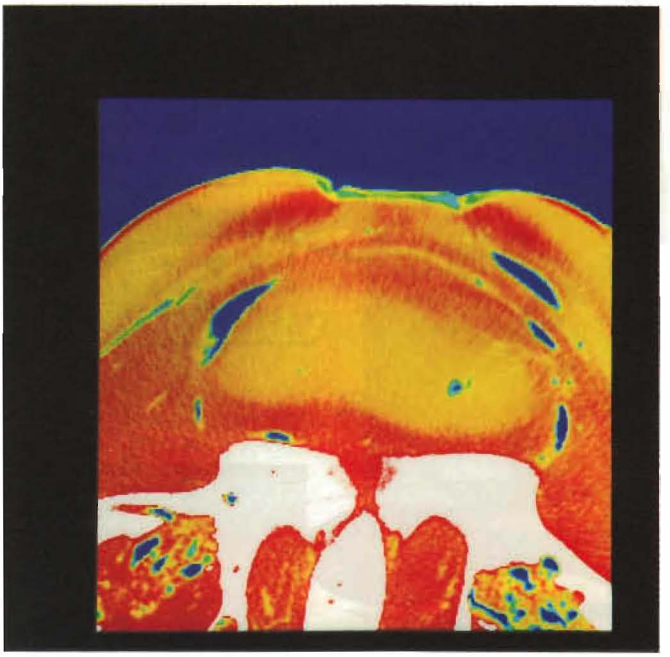

a

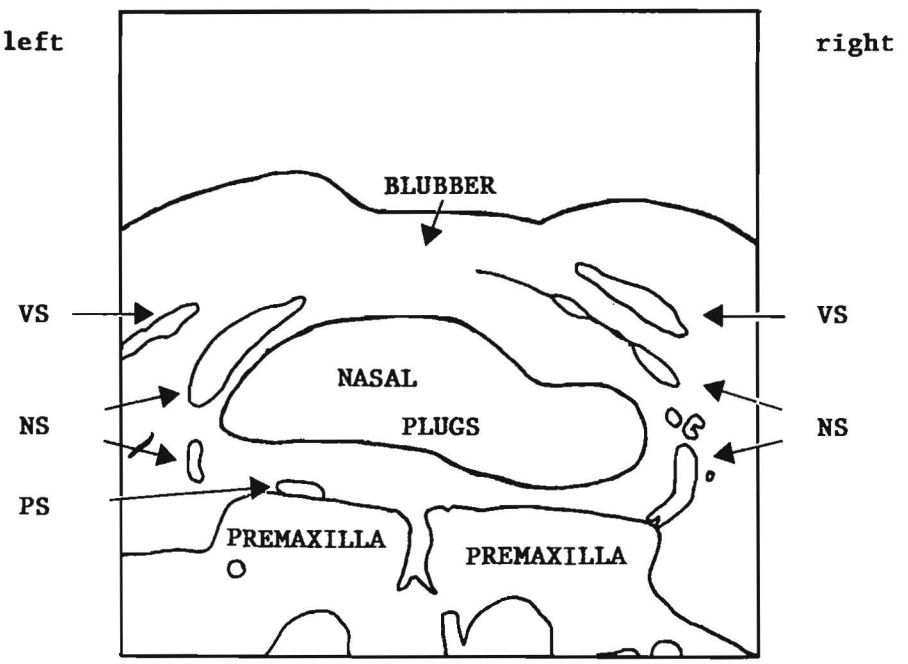


b

**Figure 6.** A typical transverse CT-image (no. 28-threshold value 850) across the nasal tract system of a *Lagenorhynchus albirostris*, and schematic drawing indicating the main areas of the CT-image. Fig. 6B. VS = vestibular sac, NS = nasofrontal sac, PS = premaxillary sac.

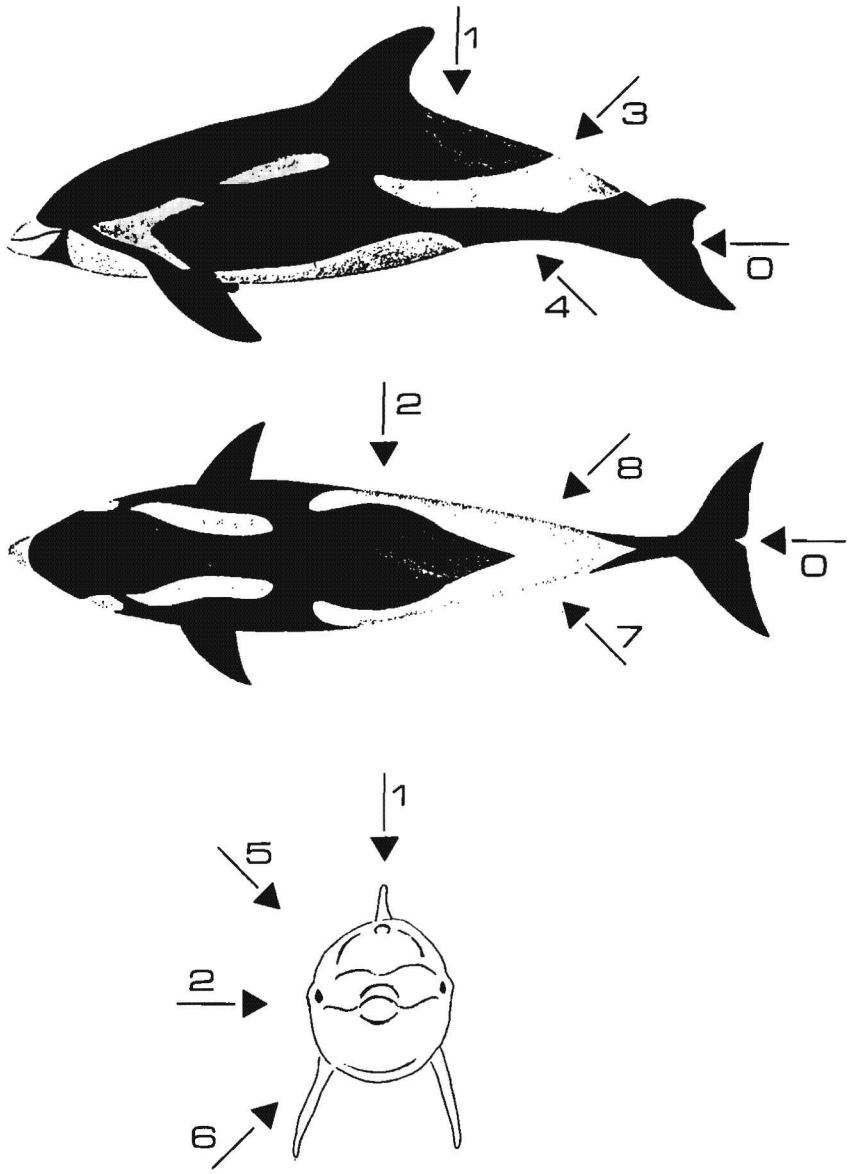


**Figure 7.** Indication of the eight standard lines-of-sight and the original line-of-sight in a lateral view, a dorsal view, and an anterior view. O = original line-of-sight.

three-dimensional configurations of the airsac system are not yet presented. However, Table 2 presents the areas and contents of the different airsacs of the *L. albirostris* numerically calculated from the scans in this research.

As an illustration of another directional line-of-sight the right vestibular sac is presented from a 45 degree angle; dorsal, right lateral (see Fig. 7, direction 5), where the segmentation in the airsac can be clearly detected (see Fig. 8).

A preliminary three-dimensional reconstruction of the same right vestibular sac is presented in Fig. 9. The number of contours is artificially doubled for better presentation by means of a linear interpolation.

**Table 2.** The surface area and contents of the investigated airsacs

| Airsac | Threshold | Surface area ($mm^2$) | Contents ($mm^3$) |
|---|---|---|---|
| Right vestibular sac | 850 | 1043.8 | 1789.6 |
| Left vestibular sac | 850 | 302.1 | 299.2 |
| Right nasofrontal sac | 850 | 2092.5 | 2816.7 |
| Left nasofrontal sac | 850 | 3230.9 | 5783.4 |
| Left premaxillary sac | 850 | 395.9 | 454.7 |

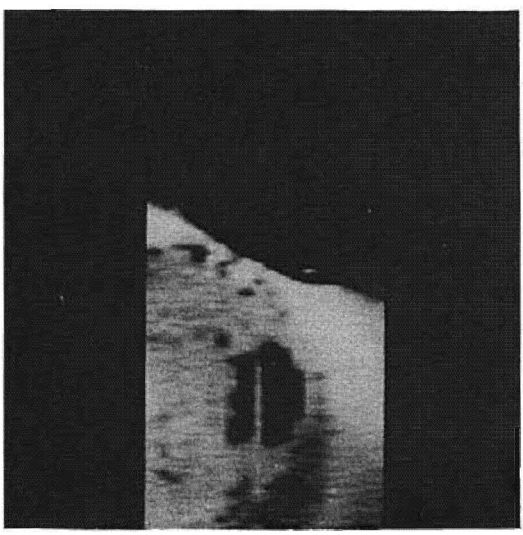

**Figure 8.** Example of a reconstruction in one of the eight standard lines-of-sight (dorso-right lateral reconstruction through pixel no. (100 225) of no. 28).

## Conclusions and Discussion

A few of the airsacs were probably not in their original form when they were scanned. The right premaxillary sac is not found in any image and the left premaxillary sac is very small. The left vestibular sac and the right nasofrontal sac are also evidently collapsed. This most likely happened during the time between death and scanning. There was a second scan session with the same dolphin, unfrozen with inflated airsacs. The analysis of this session has not yet been completed and will be discussed in a later paper.

The nasal tract region of Lagenorhynchus albirostris has been investigated and described before by Schenkkan (1973) & Parry (1978).

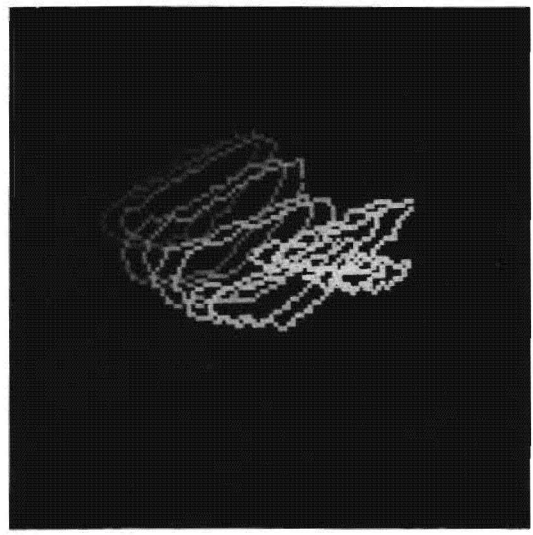

**Figure 9.** Example of a three-dimensional reconstruction of the right vestibular sac of a *Lagenorhynchus albirostris*. The number of contours is doubled by linear interpolation.

**Table 3.** Dimensions of a *Lagenorhynchus albirostris* given by Parry (1978)

| | Length (mm) | Width (mm) |
|---|---|---|
| Length dolphin | 2560 | |
| Blowhole | 50 | 40 |
| Right vestibular sac | 100 | 75 |
| Left vestibular sac | 70 | 40 |
| Right nasofrontal sac | 110 | 45 |
| Left nasofrontal sac | 60 | 20 |
| Right connecting sac | 20 | 4 |
| Left connecting sac | 15 | 4 |
| Right nasal plug | 130 | 70 |
| Left nasal plug | 115 | 55 |

Schenkkan (1973) gave the following morphological description of the nasal tract region of *L. albirostris*:

'The vestibular sacs were very large and situated caudal and lateral to the nasal passage. The ventral walls of these diverticula were thicker than the dorsal walls . . . The nasofrontal sacs consisted of tubular caudal portions sloping dorsally along the nasal bones, their walls possessing small appendices. The rostral sections consisted of large bladder-like extensions occupying the whole area between the nasal passage and the melon. Small appendices were found in the dorsal walls of these extensions. The accessory sacs were very large and both possessed a caudal part posterior to the

orifice to the nasal passage ... The width of the premaxillary sacs in the adult constituted 40% of the total maxillary width.'

Parry (1978) gave the following description of the nasal tract region of a specific adult female dolphin (stranded alive at Hartlepool on 15 April 1976):

'The blowhole lips were coloured uniformly black. The vestibular sacs lay at right angles to the vestibule, being partially non-pigmented and grey. The effect was a somewhat mottled lining to the sacs with the characteristic corrugations of the sac linings. The right sac was larger than the left ... The inferior vestibules and the tubular sacs contained raised mounds indicating the presence of glands. The diameters of the duct openings, including the raised epithelium surrounding them, was 2 mm ... The tubular sacs were grey pigmented with large areas of white coloured epithelium, particularly the anterior limbs ... The expansion of the anterior limb of the right tubular sac is much more pronounced and twice as long and wide as the left.'

Table 3 presents the dimensions of this dolphin.

It is difficult to compare the dimensions found by Parry (see Table 3) with those found in this research (see Table 2). An airsac does not have a simple shape, which means that an unambiguous length and width is difficult to define. It is even more difficult to translate length and width into the area and contents of a region.

The airsacs of the dolphin scanned in this study probably did not have their original, air-filled shape. This means that the sizes calculated will be smaller than the true area and contents. Since the collapse of the airsacs had no connection with the scanning, other techniques would also have suffered from this problem.

One advantage of x-ray computer tomography over dissection is the possibility of re-using the images. As soon as a new point of interest is found, new searches can be made and new viewpoints studied in all previously made images. Another advantage is that the CT-scanner does not damage the specimen, which means that the animals can still be used for other experiments or for dissection. A disadvantage is that the material can not be seen in actuality, so the colour and the texture of the tissue cannot be described as Parry (1978) described them. Using different techniques on the same specimen can clarify the advantages and disadvantages of the various techniques and may lead to a solution to the problem of the sonar source.

The experiments described here use simple image processing techniques to distinguish the region of interest from its surroundings. In principle, all regions can be found by using an upper and a lower threshold. Air that has the lowest possible Hounsfield value only requires an upper threshold; bone, having the highest possible Hounsfield value, only requires a lower threshold. All the other tissues require two thresholds.

When the Hounsfield values of a region of interest differ very little from their surroundings (e.g. when distinguishing white and grey brain tissue), noise can make finding the right contour more difficult. The noise can make the value of a pixel a bit higher or lower and give the pixel a value in the range of the opposite tissue. More powerful methods may be necessary to select the region then. These methods are already used in other fields of research.

When the contour of a region is found, it is easy to calculate the size. In anatomy, it is difficult to calculate the area and contents. By using CT-images, this can be done easily and accurately. The elongatedness and dispersedness have been calculated as they also are important in clarifying the role of the nasal tract region in sound production. Apart from these shape characteristics other shape characteristics can be calculated. The chain code contains some useful shape information. For example, the frequency with which each code is used is counted and when a peak appears for a certain code, an indication is given for the direction of the region. Differences between two successive codes give information about the smoothness of the contour, while many large changes means a relatively wrinkled contour. Characteristics like length, the largest distance between two contour pixels, can be interesting, but they are difficult to calculate because more images are involved.

Information from individual images is often difficult to place in the total system. Combining information from different images and making a three-dimensional reconstruction can help to give a more useful overview. A good impression can be gained particularly when three-dimensional reconstructions from different viewing points are made.

The possibilities of combining information obtained from images are numerous. One special region can be studied, but influences between regions can also be studied. If each region is allocated its own colour, they will be easy to separate in a three-dimensional reconstruction. In this way, a vivid impression of a whole area can be brought about. When data are collected from reconstructions in different directions, valuable information about shapes and distances between regions can be obtained. This information will be indispensable in providing conclusive confirmation for any hypothesis concerning sound production in odontocetes and in other still unsolved problems in cetology.

**Acknowledgements**

The authors are highly indebted to Dr P. J. H. van Bree of the Institute of Taxonomic Zoology, University of Amsterdam, for providing the White-beaked dolphin, and to Frans J. Engelsma and his staff of the Ouwehand Zoo, Rhenen, for their support in the transportation of the animal outside

working hours. The assistance of F. van der Meer, MSc of the Radiodiagnostics Group, EUR, with the image transfer into our VAX-system is highly appreciated, and last, but not least we acknowledge the magic of J. H. Verschuur in producing the colour cross section in figure 6.

## References

Alcuri, G. (1980) The role of cranial structures in odontocete sonar emission. In: Animal Sonar Systems, ed. R. G. Busnel & J. F. Fish, Plenum Press, New York: 847–451.

Cranford, T. W. (1988) The anatomy of acoustic structures in the spinner dolphin forehead as shown by x-ray computed tomography and computer graphics. In: Animal Sonar Processes and Performance, ed. P. E. N. Nachtigall & P. W. B. Moore, Plenum Press, New York: 67–77.

Dormer, K. J. (1979) Mechanism of sound production and air recycling in delphinids: Cineradiographic evidence, *J. Acoust. Soc. Am.* **65(1),** 229–240.

Evans, W. E. & Maderson, P. F. A. (1973) Mechanisms of sound production in Delphinid cetaceans: a review and some anatomical considerations, *Amer. Zool.* **13,** 1205–1213.

Evans, W. E. & Prescott, J. H. (1962) Observations of the sound production capabilities of the bottlenose Porpoise; A study of whistles and clicks. *Zoologia, New York,* **47,** 121–128.

Green, R. F., Ridgway, S. H. & Evans, W. E. (1980) In: Animal Sonar Systems, ed. R. G. Busnel & J. F. Fish, Plenum Press, New York: 204.

Kak, A. C. & Slaney, M. (1988) Principles of Computerized Tomographic Imaging, IEEE Press, New York.

Lawrence, B. & Schevill, W. E. (1956) The functional anatomy of the delphined nose, *Bulletin of the Museum of Comparative Zoology at Harvard College*, Cambridge, U.S.A., **114(4),** 103–151.

Mackay, R. S. & Liaw, H. M. (1981) Dolphin Vocalization Mechanisms, *Science,* **212,** 676–678.

Norris, K. S. (1964) Some problems of echolocation in cetaceans. In: Marine bio-acoustics, ed. W. N. Tavolga, Pergamon Press, 317–336.

Norris, K. S., Harvey, G. W., Burzell, L. A., Kartha, K. (1972) Sound production in the Freshwater Porpoises *Sotalia cf. fluviatilis* Gervais and Deville, and *Inia geoffrensis* Blainville, in the Rio Negro, Brazil, *Investigations on Cetacea*, Vol. IV, Berne: 251–259.

Parry, K. (1978) The functional anatomy of the odontocete nose and snout, Ph.D. Thesis, Girton College, Cambridge, England.

Pilleri, G. E. (1979) Sonar Field Pattern in Cetaceans, Feeding Behaviour and the Functional Significance of the Pterygoschisis, *Investigations on Cetacea*, Vol. X, Berne: 147–155.

Purves, P. E. & Pilleri, G. E. (1978) Functional anatomy and general biology of *Pseudorca crassidens* (OWEN) with a review of the hydrodynamics and acoustics in cetacea, *Investigations on Cetacea*, Vol. IX, Berne: 155–186.

Ridgway, S. H., Carder, D. A., Green, R. F., Gaunt, A. S., Gaunt, S. L. L. & Evans, W. E. (1980) Electromyographic and pressure events in the nasolaryngeal system of dolphins during sound production. In: *Animal Sonar Systems*, ed. R. G. Busnel & J. F. Fish, Plenum Press, New York: 239–250.

Rosenfeld, A. & Kak, A. C. (1982) *Digital Picture Processing*, Vol. 2, Academic Press, London.

Schenkkan, E. J. (1971) The occurrence and position of the 'connecting sac' in the nasal tract complex of small odontocetes. Beaufortia, Volume **19(246)** pp. 37–43.

Schenkkan, E. J. (1972) On the nasal tract complex of *Pontoporia blainvillei, Investigations on Cetacea*, Vol. IV, Berne: 83–90.

Schenkkan, E. J. (1973) On the comparative anatomy and function of the nasal tract in odontocetes, Bijdragen tot de dierkunde **43(2):** 127–160.

Schenkkan, E. J. (1977) Notes on the nasal tract complex of the Boutu, *Inia geoffrensis*, Bijdragen tot de dierkunde **46(2):** 275–283.

Schenkkan, E. J. & Purves, P. E. (1973) The comparative anatomy of the nasal tract and the function of the spermaceti organ in the physeteridae (mammalia, odontoceti), Bijdragen tot de dierkunde **43(1):** 93–113.

Vossepoel, A. M. & Smeulders, A. W. M. (1981) Statistical properties of digitised line segments. In: Computer Graphics 81 (Conf. Proc., London, Oct. 27–29, 1981) Northwood UK: Online: 471–483.